In Vitro Bacterial Growth on Titanium Surfaces Treated with Nanosized Hydroxyapatite

Maria Holmström *, Sonia Esko , Karin Danielsson , Per Kjellin

Posted Date: 30 December 2024

doi: 10.20944/preprints202412.2525.v1

Keywords: nanosized hydroxyapatite; implant; surface coating; antibacterial; biofilm; S. epidermidis; P. aeruginosa

Article

In Vitro Bacterial Growth on Titanium Surfaces Treated with Nanosized Hydroxyapatite

Maria Holmström [1]*, Sonia Esko [2], Karin Danielsson [1] and Per Kjellin [1]

[1] Promimic AB, Entreprenörsstråket 10, 431 53 Mölndal, Sweden
[2] Chalmers University of Technology, Department of Applied Chemistry, 412 96 Göteborg, Sweden
* Correspondence: maria.holmstrom@promimic.com

Abstract: Bacterial growth on implant surfaces poses a significant problem to the long term success of dental and orthopedic implants. There is a need for implant surfaces which promote osseointegration, while at the same time decreasing or preventing bacterial growth. In this study, we adapted existing methods for measurement of bacterial biofilms, to be suitable for measuring the bacterial growth on implant surfaces. We used two different strains of bacteria, *Pseudomonas aeruginosa* and *Staphylococcus epidermidis*, and investigated the in vitro effect of bacterial growth on titanium surfaces coated with an ultrathin (20–40 nm thick) layer of nanosized hydroxyapatite (HA). We found that after 2 hours of biofilm growth, there was a 33% reduction of bacteria for both *S. epidermidis* and *P. aeruginosa* on nanosized HA compared to Ti. For a more mature 24 h biofilm, there was a 46% reduction for *S. epidermidis* and a 43% reduction for *P. aeruginosa* on nanosized HA compared to Ti. This shows that nanosized HA can be of benefit in reducing implant related infections, together with antimicrobial therapy.

Keywords: nanosized hydroxyapatite; implant; surface coating; antibacterial; biofilm; *S. epidermidis*; *P. aeruginosa*

1. Introduction

The use of dental and orthopedic implants is steadily increasing. A highly undesirable phenomenon in implant surgery is infection at the implantation site. Surgical site infections are troublesome with increased patient morbidity and mortality, longer hospital stays and increased healthcare costs. The treatment is even more demanding in relation to implants and can in worst case lead to implant rejection. Infections may be classified as either early onset or late onset, but the border between these phases varies in literature, anywhere from 30 days to 2 years post-surgery are classified as late infections [1–7].

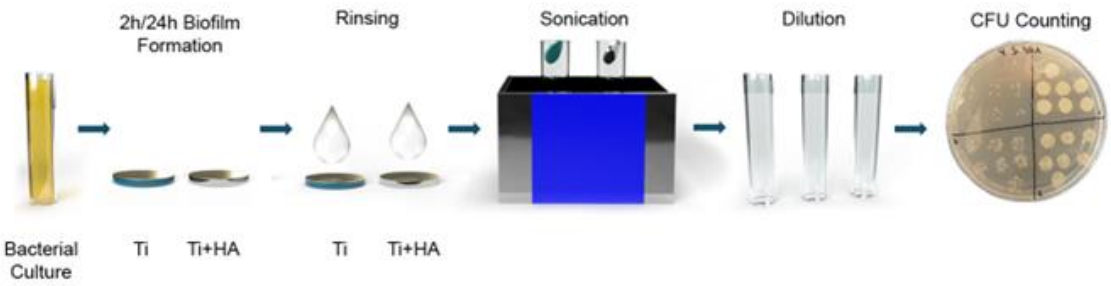

Bacterial strains which are known to cause infections in orthopedic implant surgery include coagulase negative staphylococci such as *S. epidermidis*, *S. aureus*, streptococci, *P. aeruginosa*, *E. coli*, enterococci, *Cutibacterium* species and *Enterobacter* species [4–6,8,9]. Early infections often arise due

 doi:10.20944/preprints202412.2525.v1

to direct inoculation during surgery, whereas late onset infections occur via hematogenous spread [6,8]. Generally, early infections are caused by more virulent bacterial strains whereas late infections are due to more low-virulent strains [7,8].

The risk of human staphylococcal infection has been shown to be more than 10 000 fold increased in presence of a foreign body [10] and in a guinea pig infection model, an inoculum of *S. aureus* was lowered to as little as 100 Colony Forming Units (CFU) in the presence of subcutaneous implants, whereas 10^8 CFU could be cleared by the immune system without signs of infection in absence of a foreign body [11]. A lowered bacterial number to cause infections in presence of implants is also observed in other animal infection models, as well as in patients [12–15]. This may be due to several factors, in addition to the immune response and frustrated phagocytosis associated with implants. Biofilm bacteria can alter the immune response to evade elimination using quorum sensing molecules [16]. Staphylococcal biofilms have been shown to drive the immune response into an anti-inflammatory and fibrotic response and alter both neutrophil and macrophage function [16–19]. The immune response also alters depending on implant topography and bacterial species present [20].

Infection rates depend on patient factors, surgery procedures and hygiene routines [21] as well as implant design [22]. Antibiotic treatment, both systemic and local, is one strategy to reduce infection rates. Another approach is to modify the implant surface. One can distinguish two different methods to combat bacterial growth on an implant surface: the bacteriostatic and the bactericidal. Both approaches are commonly used together. In the bacteriostatic approach, the surface prevents growth of bacteria. This can be achieved by creating superhydrophilicity [23], surface topographical changes and by applying antifouling coatings such as polymer brushes [24]. A smoother surface lowers the surface area and thereby decreases the amount of attachment points for the bacteria [25]. This method is used for external fixation pins [26] and dental abutments [22]. However, in patients, many factors are influencing the risk of implant infections, and a significant difference between smooth, moderately rough and rough surfaces when it comes to biofilm formation and peri-implantitis are not always observed [27,28].

The bactericidal approach is to modify the implant surface to kill bacteria. Noble metal coatings [29,30], coatings containing antibiotics [31] and hydrogels [32] have been successfully used to create a bactericidal effect, as has the use of quaternary ammonium compounds [33] and nanopatterning of the surface, such as creating nano-pillars and -pores [34].

Apart from infection, insufficient bone-to-implant integration is another factor increasing the failure rate of dental and orthopedic implants, and to improve this, the properties of the implant surface are of vital importance. Factors such as micro roughness, nano roughness, chemical composition and physical and mechanical factors all affect osseointegration [35]. However, the factors that are known to affect osseointegration are often similar as the properties which affect bacterial growth, especially regarding surface texturing techniques. Making an implant surface rougher by blasting and/or acid etching is known to promote osseointegration, but also provides a great substrate for bacterial growth. Conversely, a polished smooth surface which displays a low bacterial growth rate often has poor osseointegration. Ideally, an implant surface should display a fast osseointegration, and also have antibacterial properties, and the challenge is naturally to combine these properties.

Hydroxyapatite (HA) coatings are well known to improve implant osseointegration [36,37]. Thick (> 50 μm) plasma sprayed HA was introduced on orthopedic implants in the 1980s, with a significant effect on implant integration. In later years, some concerns have been raised on clinical problems with thick HA coatings, such as delamination and wear [38,39] and thinner coatings can be better in stimulating osseointegration without these risks. Implant treatment with ultrathin coatings of nanosized HA is known to have a significant effect on osseointegration [40,42], even in compromised bone [43,44]. However, the effect on bacterial growth on nanosized HA is not well studied.

There are many different ways to study bacterial biofilm growth, including static and flow cell models, culturing and microscopy studies. Due to simplicity, surface coated discs are often coated on

 doi:10.20944/preprints202412.2525.v1

one side, placed in well plates or flasks for biofilm growth and then biofilm removal is made using ultrasound treatment. However, for this procedure the question arises of what is growing on the non-coated part of the disc. This may impose a problem, and coating of both sides of the discs is not always a viable option.

The aim of the current study was therefore to refine existing methods to investigate bacterial growth on surfaces, and to use this method to investigate the bacterial growth on Ti substrates, with or without a coating of ultrathin (20–40 nm) nanosized hydroxyapatite. For this purpose, a drop method was used, placing a bacterial drop onto discs for growth. In addition, a well plate was created to press onto Ti and nanosized hydroxyapatite modified Ti disc, only to expose the top surfaces to bacteria. Below the Ti discs a bottom plate was placed, and everything was held together by screws. A bacterial count of $1{\cdot}10^6$ or 50 000 CFU/ml of *S. epidermidis* or *P. aeruginosa* was used and allowed to form 2 or 24 h biofilms, before biofilm removal and culturing.

2. Materials and Methods

2.1. Surface Preparation

Two types of Ti discs were used in this study: 1 cm Ø discs of Ti grade 4 and 2 cm Ø discs of Ti grade 2. The larger diameter was chosen to improve the statistics for the 24 h experiments; Ti grade 2 and grade 4 both consist of Ti, with no difference in biological response, but grade 4 has a higher mechanical strength. All discs were ground using P400 grit sandpaper, ultrasonically cleaned for 10 minutes per step using isopropanol (Fisher Scientific, 99%), 1 M HNO_3 (Scharlau, 65%), H_2O type 1 and isopropanol. The 2 cm discs were also thermally cleaned for 5 minutes in 450 °C (Nabertherm) to obtain a more homogenous HA layer. This procedure was performed for both the control discs and the discs to be coated with nanoHA. Then discs were either used as Ti controls or surface treated with nanoHA. In short, the nanoHA layer was applied through spin coating; a coating liquid containing nanosized HA was applied to the surfaces, which were then rotated and finally thermally treated at 450 °C. A more thorough description of the coating procedure and coating liquid is provided in reference [42].

2.2. Surface Characterization

SEM and EDX were done using a Zeiss FEG-SEM Sigma with Gemini optics and equipped with Energy-dispersive X-ray spectroscopy, EDX. 3 discs were studied and 3 EDX spectra were obtained for each disc, giving a total of 9 spectra for each type of disc.

24 hour bacterial biofilms as presented below were also studied in SEM. Before SEM analysis, the biofilms were left overnight in 4% buffered paraformaldehyde (VWR chemicals) and then rinsed 3 times in PBS (Sigma Aldrich, 0.01 M) before subjected to a drying gradient of 50, 60, 70, 80, 90 and 100 % ethanol (Fisher Scientific, ≥99%) for 10 minutes per step. Samples were then left in 50% hexamethyldisilazane (Thermo Fisher, 98%) in ethanol for 20 minutes and finally left in 98% hexamethyldisilazane and allowed to dry in ambient air. Before SEM analysis, the samples were gold sputtered for 60s, 10 mA (Emitech K550X).

Contact angle measurements were performed to investigate the hydrophilicity of the samples. 5µl drops of type 1 water were dropped onto the surfaces, either Ti controls or nanoHA coated Ti, photographs were obtained and contact angles were determined using the software ImageJ 1.54 g. 3 drops were tested on each surface.

2.3. Calcium Assay

A colorimetric calcium assay was performed to investigate the amount of calcium ions on the nanoHA coated surfaces, which in turn can be used to calculate the approximate thickness of the nanoHA coating. First, 12 mm nanoHA coated discs were dipped in 5 ml 0.01 M HNO_3 (Scharlau, 65%) for 5 minutes; this procedure dissolves all HA which is present on the disc. Then, 5 ml of a solution consisting of 60 µM ArsenazoIII (Sigma Aldrich) in 0.1 M Tris solution (Fisher Scientific) was added; this step increases the pH of the solution. The calcium-dye complex turned purple-red and its

 doi:10.20944/preprints202412.2525.v1

absorbance was immediately measured at 650 nm (Jenway 7315 Spectrophotometer) and compared to a standard curve.

2.4. Bacterial Strains and Culture

S. epidermidis CCUG 39508 and *P. aeruginosa* CCUG 56489 were grown on Brain heart infusion (BHI, Becton, Dickinson and Company) agar (Fisher Scientific) at 37°C, then stored in fridge. Colonies were then transferred to BHI medium and cultured overnight in 37°C, to stationary phase and used for 2 h biofilm experiments. For 24 h biofilms, overnight samples were immediately used if in mid logarithmic phase, otherwise transferred to fresh BHI and re-cultured into mid-exponential growth phase, corresponding to Abs_{600nm} between 0.5 and 0.7 (Jenway 7315 Spectrophotometer).

2.5. Biofilm Assay

Samples for 2 h biofilms were diluted to $1{\cdot}10^6$ bacteria/ml in BHI and 80 µl (80 000 bacteria) was added as a drop onto the top of 1 cm Ø discs and cultured for 2 h at 37 °C in air, before biofilm removal. The drop method enabled biofilm growth on only the coated surface, but it had limitations on how long culturing was possible, due to drying effects.

For the 24 h biofilms, 9 well metal plates were created, to culture biofilms on one side of the discs only. The well plates consisted of a top part with holes to create the wells, into which 2 cm Ti discs were fitted with a silicone O-ring. Below the discs a silicone sheet was fitted to maintain the liquid inside the wells, then a Teflon plate and finally a solid metal bottom plate, all of which was held together by screws, see Figure 1. For these tests, 2 cm discs were used instead of 1 cm to increase biofilm surface areas and statistics.

Log phase bacteria for 24 h studies were ultrasonically homogenized, 10 s, 20% power (Bandelin Sonopuls, Probe MS72) and diluted to 50 000 bacteria/ml in BHI, using a Bürker Türk counting chamber and optical microscope (Zeiss Axioskop 40). 1 ml was added to each disc and cultured for 24 h at 37 °C in air.

Figure 1. Assembled 9-well plate.

After growth, discs were rinsed in 1 ml PBS (0.01 M, Sigma Aldrich), and 1 cm discs were transferred to 1 ml fresh PBS and 2 cm discs were transferred to 2 ml PBS. For 24 h *P. aeruginosa*, discs were pipetted 5 times to remove visible biofilm from the discs. Then, all discs were ultrasonicated for 5 minutes (Elmasonic S 80H, 37 kHz) for biofilm removal. Due to presence of visible bacterial lumps, 24 h *P. aeruginosa* solutions were then ultrasonically homogenized for 10 s at 20% power (Bandelin Sonopuls, Probe MS72), to dislodge large bacterial aggregates. Bacterial solutions were then serially diluted in PBS and 7*10 µl drops per dilution were cultured on BHI agar plates at 37 °C in air overnight, according to the drop plate method. 17 different 2 h triplicate biofilm experiments were

 doi:10.20944/preprints202412.2525.v1

done, yielding a n-value of 51. For the 24 h biofilms, 8 experiments were done in triplicates or quadruplicates, yielding an n-value of 30.

2.6. Confocal Microscopy

The confocal microscope used was a ZEISS LSM 980 with Airyscan 2. Samples were stained using LIVE/DEAD *Bac*Light, kit L13152 (Invitrogen), utilizing propidium iodide and Syto 9, prepared according to the manufacturer. 10 µl was added to each disc and incubated in the dark in room temperature for 15 minutes before observation.

2.7. Statistical analysis

A two-sided student's t-test for unpaired samples of unequal variance was utilized for statistical analysis. Any p-value below 0.05 was considered statistically significant.

3. Results

3.1. Surface Characterization

SEM images of 1 and 2 cm discs of pure Ti and nanosized HA coated Ti are shown in Figures 2 and 3. At 500X magnification, both surfaces looked smooth whereas at 40 000X magnification the nanosized HA treated Ti was shown to be covered in hydroxyapatite crystals. The crystal size was estimated from SEM imaging to be 100 ± 20 nm in length and 6 ± 2 nm wide. This was in similar range to previous studies [42,45]. The 12 mm nanocoated discs used for the calcium assay is seen in Figure 4 and show the same nanoHA crystals and similar coverage as the other discs.

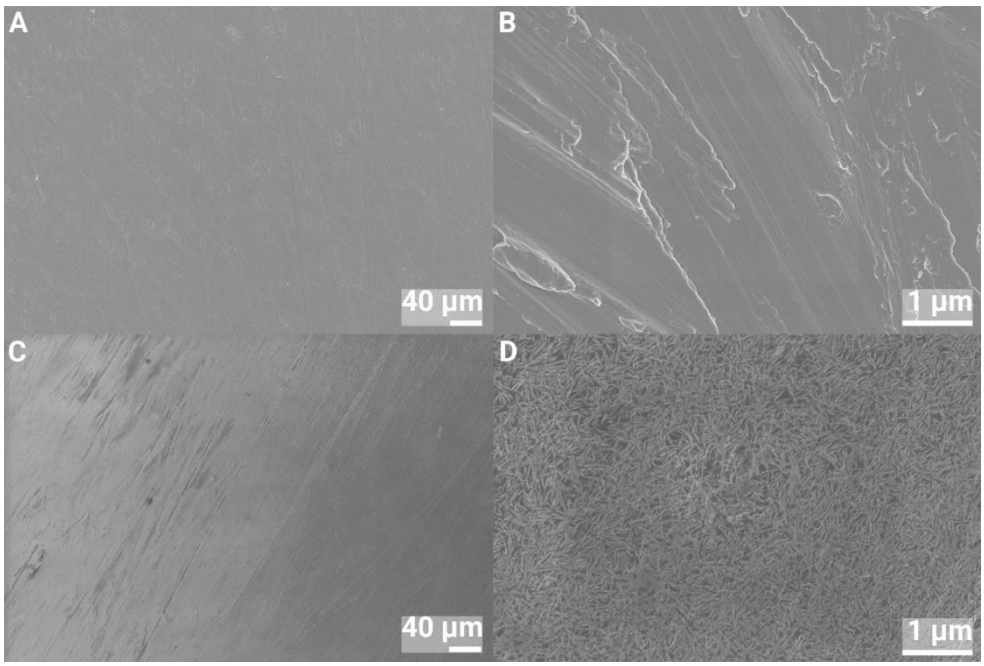

Figure 2: SEM images of 1 cm Ti discs (A, B) and Ti with nanosized HA coating (C, D) at 500X (A,C) and 40000X (B,D) magnification**.**

 doi:10.20944/preprints202412.2525.v1

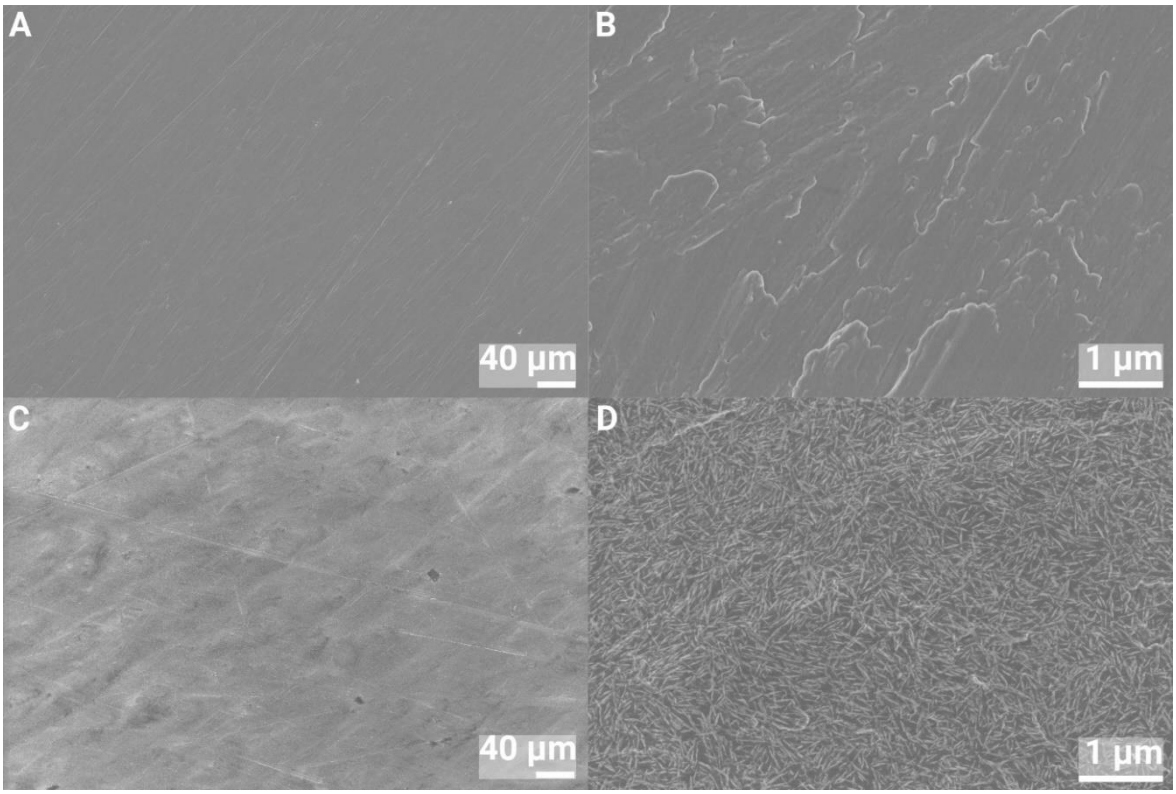

Figure 3. SEM images of 2 cm Ti discs (A, B) and Ti with nanosized HA coating (C, D) at 500X (A,C) and 40 000X (B,D) magnification.

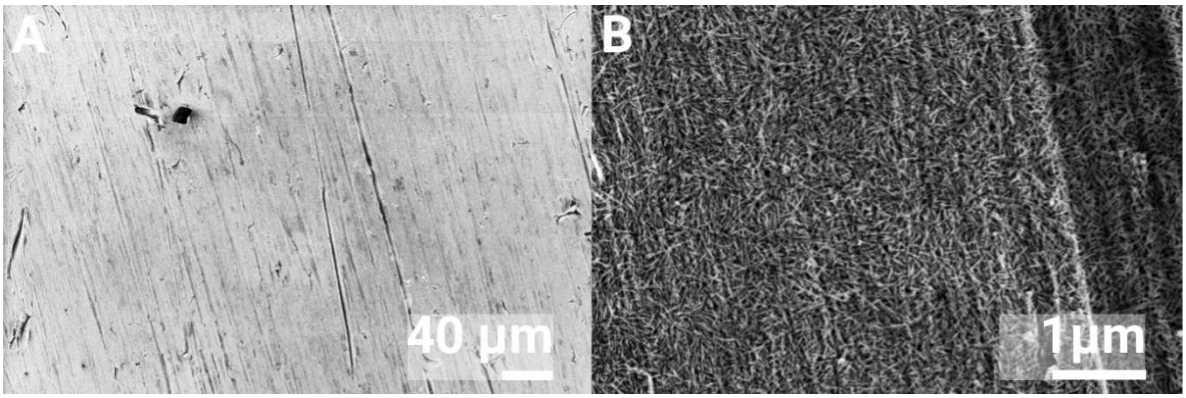

Figure 4. SEM images of nanosized HA coating on discs used for Ca assay, at 500X (A) and 40 000X (B) magnification.

EDX data, see Table 1, showed the elemental composition of HA treated Ti grade 4 to contain 0.42% calcium and 0.32% phosphorus, in addition to titanium, oxygen and carbon whereas the grade 2 discs contained 0.25% calcium and 0.19% phosphorus. An increase in oxygen content for the heat treated discs was also observed, this effect is most likely due to an increase in TiO_2 layer thickness.

Table 1. EDX analysis of Ti and nanosized HA coated Ti of grade 2 and 4 (atomic percent).

Element	C	O	Ti	Ca	P
Ti grade 4	3.13±0.23	12.90±0.45	83.97 ± 0.61	-	-
nanoHA, Ti grade 4	2.06±0.25	28.09±1.09	69.11 ± 1.58	0.42±0.15	0.32±0.13

 doi:10.20944/preprints202412.2525.v1

Ti grade 2, heated 450 °C	2.65±0.13	25.61±1.41	71.74±1.46	-	-
nanoHA, Ti grade 2	1.75±0.19	30.09±1.25	67.72±1.28	0.25±0.04	0.19± 0.05

The calcium assay was performed on 8 discs and gave an average calcium ion content of 3.2 μg/cm^2. With a HA molecular weight of 502.31 g/mol this corresponds to 8 μg HA/cm^2. Assuming a solid layer and a density for HA of 3.15 g/cm^3, a rough estimate of the layer thickness can be estimated. A HA content of 8 μg/cm^2 then yields a thickness of 25 nm.

The contact angle measurements showed the nanosized HA coated Ti to be superhydrophilic (contact angle < 10 °), whereas the Ti controls were hydrophilic with a contact angle of 39° for 1 cm Ti discs and 53° for 2 cm Ti discs, see Figure 5.

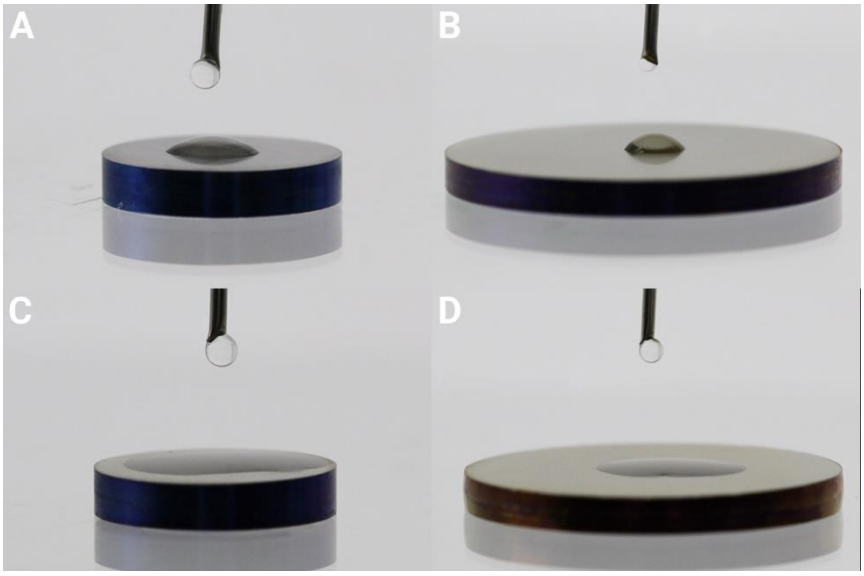

Figure 5. Contact angle of 1 and 2 cm discs, control Ti and nanoHA coated Ti.

3.2. Confocal Microscopy

Ultrasound removal of bacteria from surfaces has shown superior results for biofilm removal [46,47] but one concern in this study was that bacterial removal was insufficient, which would lead to measurement errors. If bacteria would stick harder to the nanosized HA treated surfaces compared to the Ti surfaces, less bacteria would then be cultured and hence an erroneous, lower number of bacteria would be the result. Confocal Laser Scanning microscopy (CLSM) was therefore performed to investigate the efficiency of the ultrasonic removal of biofilms, from the control Ti and nanoHA coated Ti. Images were obtained before and after ultrasound treatment for 5 minutes, 37 kHz. The control samples, that were not ultrasound treated, showed 24 h biofilms of *S. epidermidis* or *P. aeruginosa* covering the substrates, see Figure 6 and 7, where green bacteria were alive and red bacteria were considered dead or membrane compromised. After the ultrasound treatment, most bacteria were removed from both Ti and nanosized HA. However, it was observed that slightly more bacteria were present on the ultrasound treated nanosized HA compared to the Ti, but most of the retained bacteria were dead and would thus not affect the culturing results. Dead or compromised bacteria may have attached and deformed on the surface and thus they are sticking harder to it.

 doi:10.20944/preprints202412.2525.v1

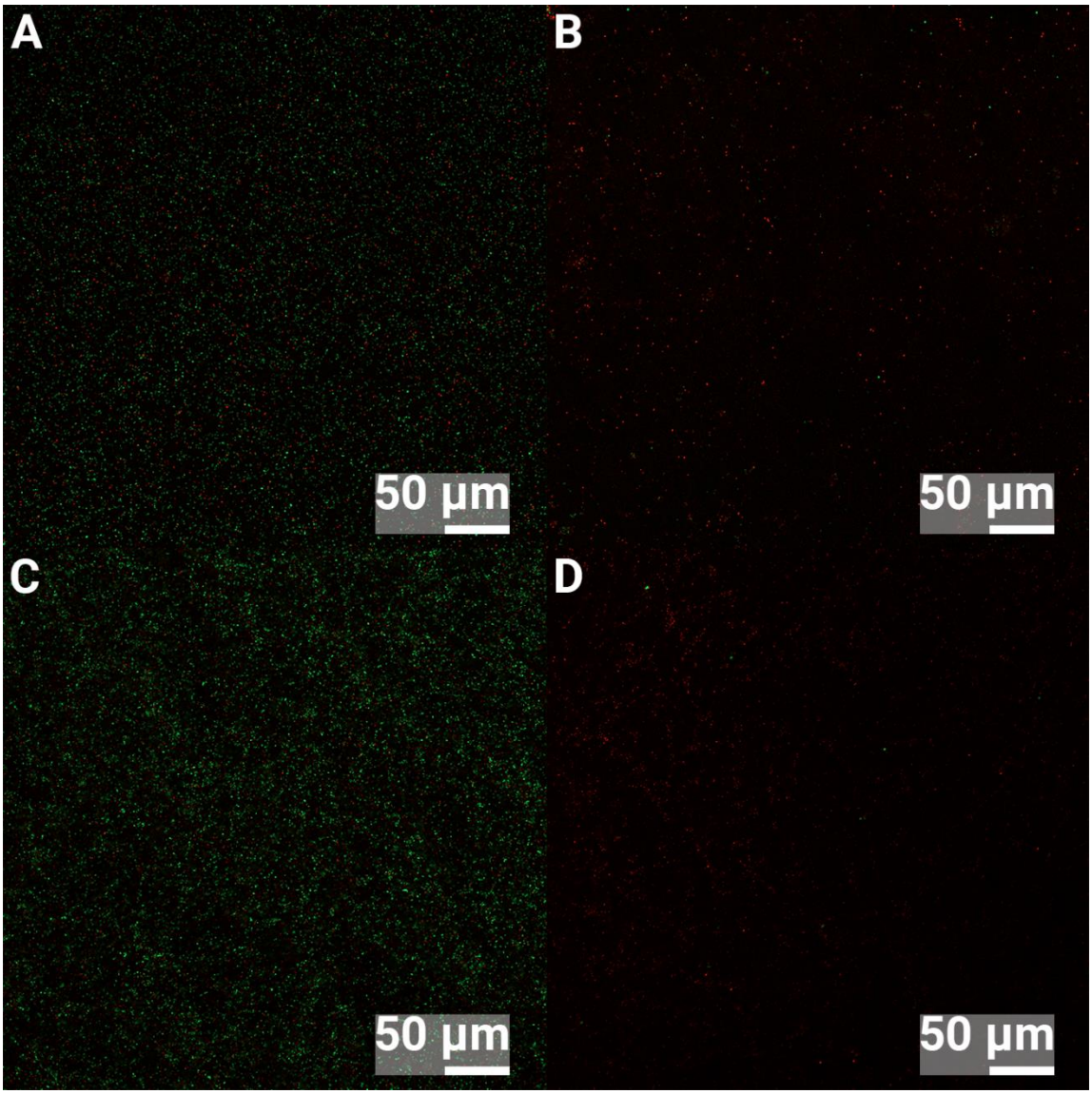

Figure 6. CLSM images of 24 h biofilms of *S. epidermidis*. A shows Ti and no ultrasound treatment, B shows Ti and 5 minutes ultrasound treatment, C shows nanoHA and no ultrasound treatment, D shows nanoHA with 5 minutes ultrasound treatment. Green bacteria are live and red bacteria are dead.

 doi:10.20944/preprints202412.2525.v1

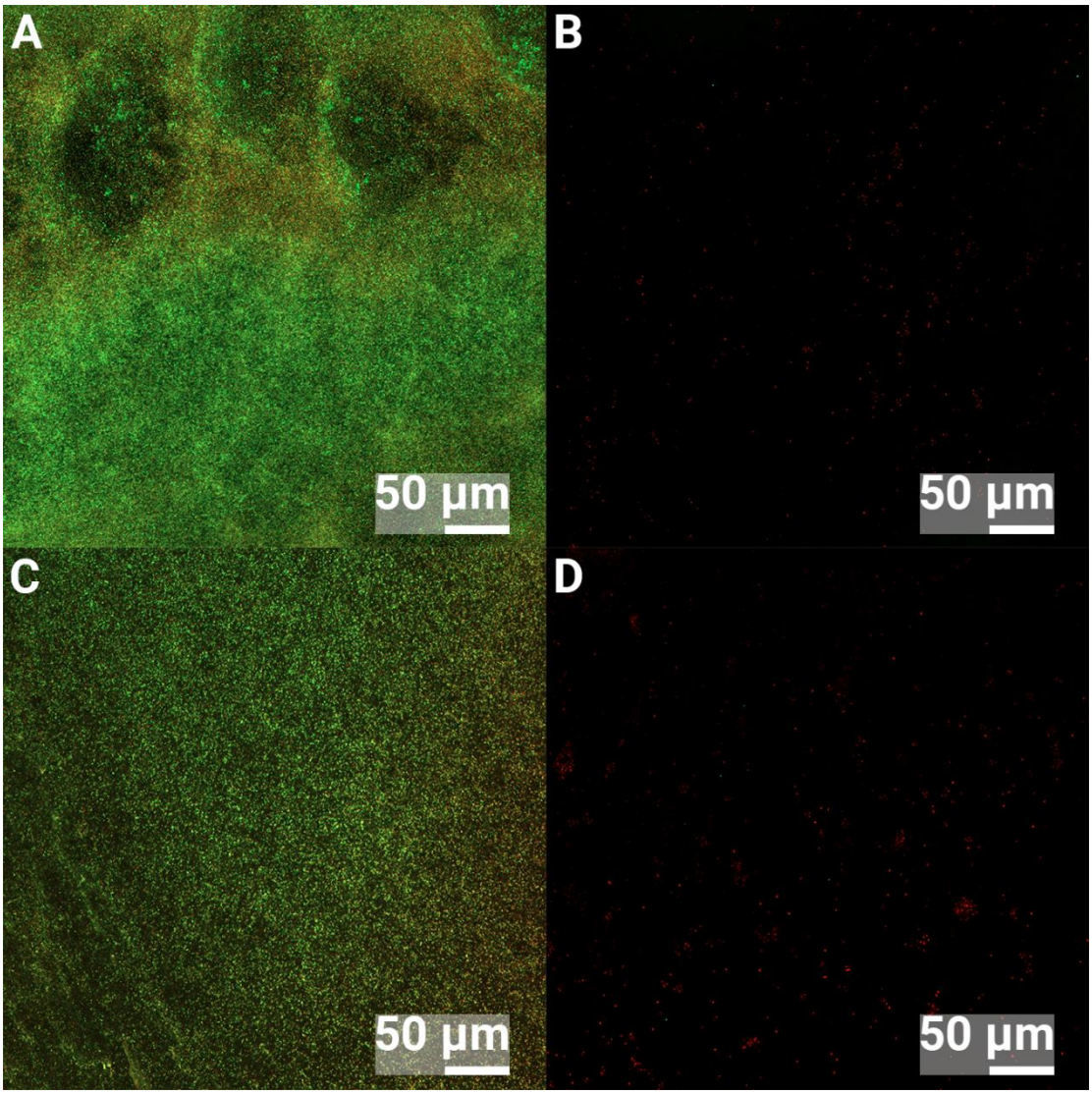

Figure 7. CLSM images of 24 h biofilms of *P. aeruginosa*. A shows Ti and no ultrasound treatment, B shows Ti and 5 minutes ultrasound treatment, C shows nanoHA and no ultrasound treatment, D shows nanoHA with 5 minutes ultrasound treatment. Green bacteria are live and red bacteria are dead.

3.3. Biofilm Assay

To investigate the potential action of the nano sized HA, both early and more mature biofilms were studied when using a biofilm assay. For the 2 h biofilms, a drop of bacteria was added to the top surface of the Ti disc. This setup was performed to prevent any misleading results from bacteria adhering to the sides and bottom of the discs that had no HA treatment, as is the case when placing discs in well plates and adding bacteria in the well.

As can be seen in Figure 8, for both *S. epidermidis* and *P. aeruginosa* there was a 33% reduction of bacteria on the nanosized HA treated Ti compared to pure Ti ($p = 0.007$ for *S. epidermidis* and $p = 0.033$ for *P. aeruginosa*).

Interestingly, *S. epidermidis* grew faster during the two hours than did *P. aeruginosa*, giving a rather large discrepancy in final bacterial content despite the same number of bacteria being added in the start. After 24 hours the results were reversed, with more *P. aeruginosa* than *S. epidermidis* biofilm bacteria. Studying the 24-hour biofilms, there was a statistically significant 45.5% reduction for *S. epidermidis* ($p = 0.025$), see Figure 9, and a 43.0% reduction for *P. aeruginosa* ($p = 0.013$), see Figure 10.

 doi:10.20944/preprints202412.2525.v1

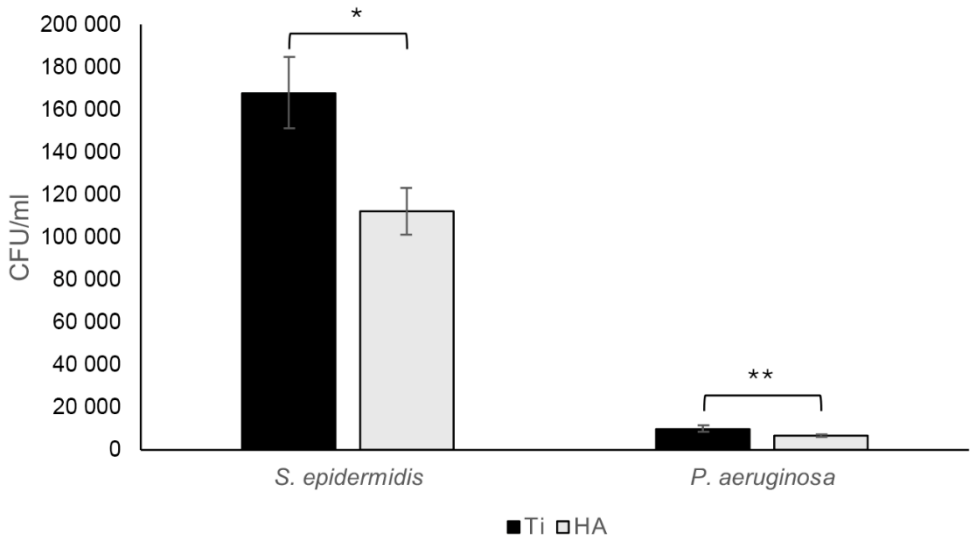

Figure 8. For 2 h *S. epidermidis* biofilms, there was a statistically significant 33.1% reduction (* p=0.007) of bacterial growth on nanosized HA compared to Ti, whereas there was a 33.0% reduction (** p=0.033) for *P. aeruginosa*. Bars show mean ± SEM.

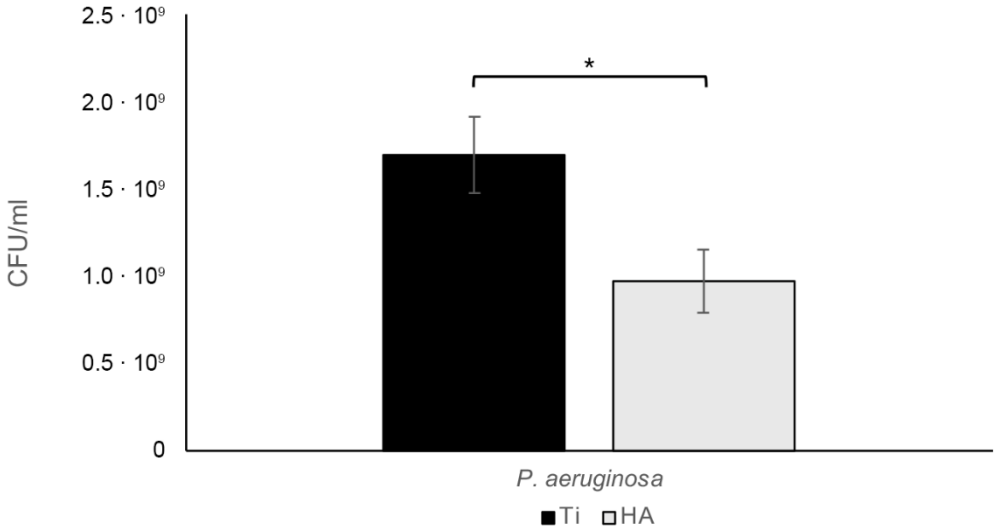

Figure 9. For 24 h *S. epidermidis* biofilms, there was a statistically significant 44.5% reduction (* p=0.025) of bacterial growth on nanosized HA compared to Ti. Bars show mean ± SEM.

 doi:10.20944/preprints202412.2525.v1

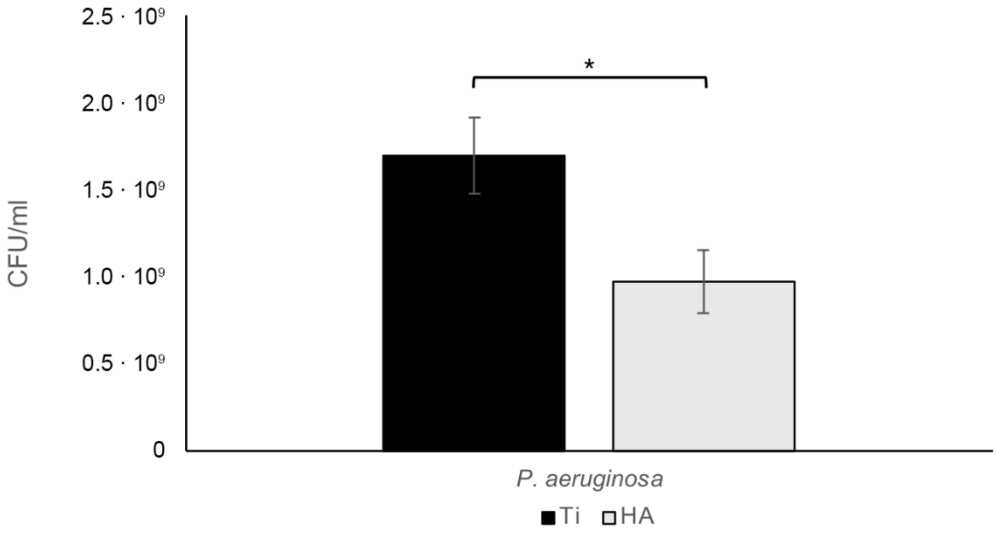

Figure 10. For 24 h *P. aeruginosa* biofilms, there was a statistically significant 43 % reduction (* p=0.013) of bacterial growth on nanosized HA compared to Ti. Bars show mean ± SEM. .

3.4. SEM of BIOFILMS

SEM analysis was done on 24 h biofilms. There were no visible differences in the appearance of individual bacteria on pure Ti compared to nanosized HA treated Ti and cell division was observed for both *S. epidermidis* and *P. aeruginosa*, see Figure 10 and 11. A few lysed bacteria were observed on the surfaces, although somewhat more lysed *P. aeruginosa* than *S. epidermidis* were found. This could be due to their thinner cell wall being more affected by the drying steps and the vacuum of the SEM. Since bacteria in general did not appear compromised, it seemed the action of the nanosized HA is bacteriostatic rather than bactericidal.

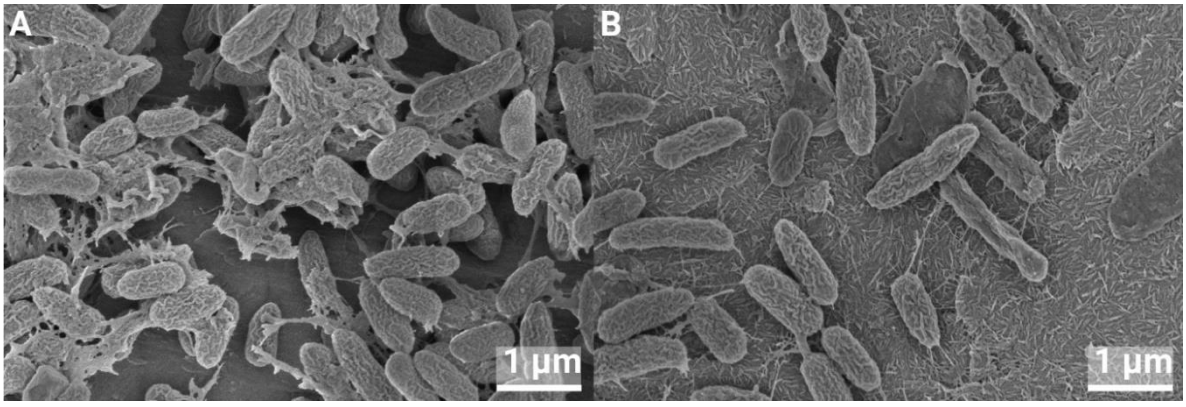

Figure 11. *S. epidermidis* growth on Ti (A) and nanosized HA treated Ti (B) for 24 h, at 40 000X magnification.

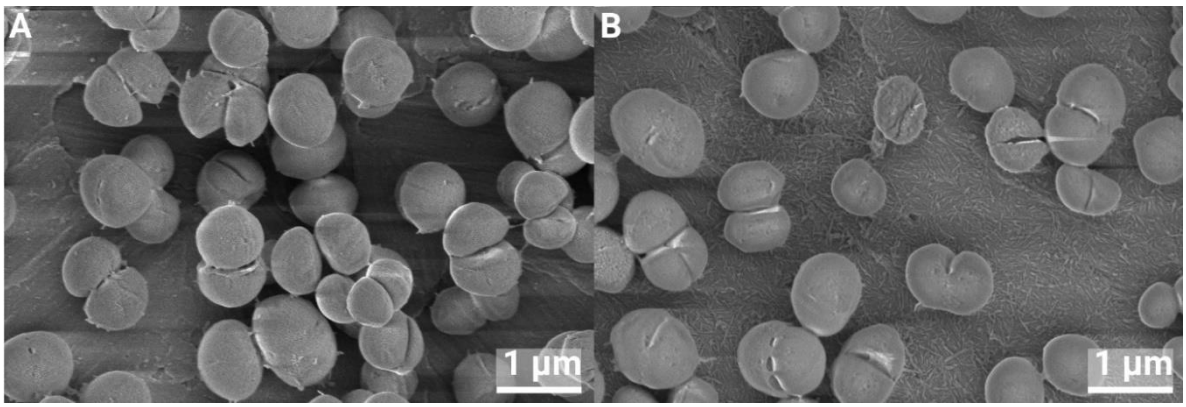

 doi:10.20944/preprints202412.2525.v1

Figure 12. *P. aeruginosa* growth on Ti (A) and nanosized HA treated Ti (B) for 24 h, at 40 000X magnification.

4. Discussion

In general, bulk HA is not regarded as an antibacterial material, but as the size of the HA crystals is decreased to the nano region, properties change. Studies using HA nanoparticles in the range of 19–200 nm demonstrated antibacterial effects against several bacterial species in planktonic phase or on agar plates, such as *E. faecalis, E.coli*, *S. aureus, Bacillus* sp. and *S. mutans* [48–51]. Nanosized HA pressed into cylindrical samples and then sintered showed antibacterial effects against *S. epidermidis*, *S. aureus* and *P. aeruginosa,* depending on sintering temperature [52]. Biofilm bacteria from pooled salivary samples showed reduced growth in presence of nanosized HA rods coated on Ti [53]. These studies showed a partial eradication of bacteria using nanosized HA, with a bacterial elimination varying from 33–46%, depending on time and species. Interestingly, the antibacterial effect was similar for both Gram positive and Gram negative bacteria, which is essential in a clinical setting where bacterial contamination may vary.

In the literature, a vast array of different kinds of nanosized HA is described, and some studies also report an increase in bacterial growth. Although antimicrobial against planktonic *C. albicans* after 24 h growth, an initial load of $1.5 \cdot 10^8$ CFU/ml of *S. mutans* and *L. rhamnosus* increased in growth when HA nanoparticles were present [54]. In this study, a large initial bacterial load was first tested but showed no antibacterial effect (data not shown). It was hypothesized that a large bacterial load crowded the surface and created a monolayer biofilm, to which new bacteria, that did not sense the surface effect, could attach. It is therefore reasonable to believe that a high bacterial load makes it difficult to distinguish the growth of bacteria in the bulk from the growth on the surface of a substrate, and the bacterial load was therefore set to a lower amount in the present study.

This lower bacterial load in in vitro studies is more clinically relevant, as the potential number of bacteria contaminating during implantation surgery is often low. Implant surgery should take place in ORs with ultraclean air, where there is ≤10 CFU/m^3 [55] and 270 CFUs attached to airborne particles has been estimated to fall down on a 250 cm^2 wound area during hip replacement [56]. Another study investigating air borne particulate contaminations during 13 hip arthroplasties showed a total CFU count of 1786, with higher numbers for longer surgery durations and higher staff counts [57]. In patients undergoing orthopedic trauma surgery, cutting the skin after disinfection and swabbing the cut yielded 4-9 000 CFUs, with a median of 8 [58] and in total knee arthroplasties the mean bacterial contamination level was 10.6 CFU/g [15]. A low initial bacterial load is also applied in many animal infection models. A rabbit spinal implant infection model using MRSA showed consistent local infection from 10^3 CFU and higher. In a similar set up, *E. coli* consistently produced infection using 10^5 CFUs. In rats, 10^6 *S. aureus* showed consistent infections in a spinal model whereas for dogs it was 10^2 CFU *S. aureus*. [14].

Intraoperative contamination during implant surgery is common, and the main sources are from the skin of the patient and airborne particles from the personnel. Even a low number of bacteria, adhering early to the implant, may interfere with the bone healing process. Both the antibacterial effect shown here and the ability of nanosized HA to osseointegrate, even in metabolically challenged patients [59], improve the odds for the immune system and antibacterial therapy to eradicate potential bacteria and prevent infections.

Attempts to find out the antibacterial mechanism of hydroxyapatite have been made for nanoparticles in solution. The most common proposed mechanism is uptake of particles by bacteria with subsequent disruption of DNA replication, formation of reactive oxygen species and direct damage to the cell membranes [60]. Another possible mechanism is dissolved calcium and phosphate ions exerting an antibacterial effect [49,60], causing damage to the cell wall and altered permeability [61,62].

Dissolution of the nanoHA coating may be one explanation to the observed bacteriostatic effect, but the SEM analysis after 24 h showed no effect on the appearance of the crystalline HA layer. Even if the crystals are still visible, some dissolution on the surface of the crystals can occur. Given that the

 doi:10.20944/preprints202412.2525.v1

total amount of Ca and P was measured to be around 8μg/cm², the amount of Ca and P from surface dissolution of the crystals will be extremely small, however. A bacteriostatic effect resulting from Ca and P release is therefore a less plausible explanation. Superhydrophilicity may be another explanation, which is well known to inhibit bacterial attachment [63], although a complete eradication of bacteria is not always obtained [23]. Yet another factor is surface charge. In physiological pH, HA is negatively charged [64], and a possible mechanism would be that negatively charged bacteria are repelled by the negatively charged HA surface. The mechanism of the antibacterial effect of the nanoHA used in this study may depend on several factors and needs further investigation.

5. Conclusions

Bacterial growth on Ti surfaces, with and without nanoHA treatment, was examined. The results of this study showed a significant antibacterial effect for surfaces coated with nanosized HA. The effect varied from 33% to 44.5% reduction, for 2 and 24 h biofilms, respectively, using *S. epidermidis* and *P. aeruginosa*, and was similar for both the gram positive and gram negative strain. In this study, a low initial bacterial load mimics the clinical settings where fewer bacteria can cause infections, and enabled detection of smaller antibacterial effects, such as the effects of nanosized HA. Although the bacterial amount is lowered, it should be emphasized that the antibacterial effect is bacteriostatic and not bactericidal; bacteria are repelled and prevented from growing, rather than destroyed. This could be of benefit since the effect appears to be physicochemical rather than biological, which reduces the risk of bacterial resistance.

Supplementary Materials: The following supporting information can be downloaded at: www.mdpi.com/xxx/s1, Figure S1: title; Table S1: title; Video S1: title.

Author Contributions: Conceptualization, MH, PK; Methodology: MH, PK; Validation MH; Formal analysis MH, SE; Investigation MH, SE, KD; Writing – original Draft Preparation MH; Writing – Review and editing PK; Visualization MH, SE; Supervision MH, PK. All authors have read and agreed to the published version of the manuscript.

Funding: This research received no external funding.

Data Availability Statement: The original contributions presented in the study are included in the article; further inquiries can be directed to the corresponding author. Data is available on request from the authors.

Acknowledgments: We acknowledge the Center for Cellular Imaging at the University of Gothenburg and the National Microscopy Infrastructure, NMI (VR-RFI 2019-00022) for providing microscope accessibility and training. Kalle Martinsson at Promimic is acknowledged for valuable help with the graphics and layout of the manuscript. Edmund Hansla at Promimic is acknowledged for valuable help with surface coating and general laboratory tasks.

Conflicts of Interest: Authors Maria Holmström, Karin Danielsson and Per Kjellin are employed by Promimic AB and owns stocks in the company. Author Sonia Esko declares no conflict of interest.

References

1. Aggarwal, V.K., M.R. Rasouli, and J. Parvizi, Periprosthetic joint infection: Current concept. *Indian J Orthop*, **2013**. *47*(1): p. 10-7. doi 10.4103/0019-5413.106884
2. Choi, S.W., et al., Clinical differences between delayed and acute onset postoperative spinal infection. *Medicine (Baltimore)*, **2022**. *101*(24): p. e29366. doi 10.1097/md.0000000000029366
3. Clark, C.E. and H.L. Shufflebarger, Late-developing infection in instrumented idiopathic scoliosis. *Spine (Phila Pa 1976)*, **1999**. *24*(18): p. 1909-12. doi 10.1097/00007632-199909150-00008
4. Parchi, P.D., et al., Postoperative Spine Infections. *Orthop Rev (Pavia)*, **2015**. *7*(3): p. 5900. doi 10.4081/or.2015.5900

5. Köder, K., et al., Outcome of spinal implant-associated infections treated with or without biofilm-active antibiotics: results from a 10-year cohort study. *Infection*, **2020**. *48*(4): p. 559-568. doi 10.1007/s15010-020-01435-2
6. Dapunt, U., et al., Surgical site infections following instrumented stabilization of the spine. *Ther Clin Risk Manag*, **2017**. *13*: p. 1239-1245. doi 10.2147/tcrm.S141082
7. Guo, G., et al., Distribution characteristics of Staphylococcus spp. in different phases of periprosthetic joint infection: A review. *Exp Ther Med*, **2017**. *13*: p. 2599 - 2608.
8. Arciola, C.R., D. Campoccia, and L. Montanaro, Implant infections: adhesion, biofilm formation and immune evasion. *Nat Rev Microbiol*, **2018**. *16*(7): p. 397-409. doi 10.1038/s41579-018-0019-y
9. Sampedro, M.F., et al., A biofilm approach to detect bacteria on removed spinal implants. *Spine (Phila Pa 1976)*, **2010**. *35*(12): p. 1218-24. doi 10.1097/BRS.0b013e3181c3b2f3
10. Elek, S.D. and P.E. Conen, The virulence of Staphylococcus pyogenes for man; a study of the problems of wound infection. *Br J Exp Pathol*, **1957**. *38*(6): p. 573-86.
11. Zimmerli, W., et al., Pathogenesis of foreign body infection: description and characteristics of an animal model. *J Infect Dis*, **1982**. *146*(4): p. 487-97. doi 10.1093/infdis/146.4.487
12. Poelstra, K.A., et al., A novel spinal implant infection model in rabbits. *Spine (Phila Pa 1976)*, **2000**. *25*(4): p. 406-10. doi 10.1097/00007632-200002150-00003
13. Laratta, J.L., et al., A Dose-Response Curve for a Gram-Negative Spinal Implant Infection Model in Rabbits. *Spine (Phila Pa 1976)*, **2017**. *42*(21): p. E1225-e1230. doi 10.1097/brs.0000000000002205
14. Wang, Y., et al., Animal Models for Postoperative Implant-Related Spinal Infection. *Orthop Surg*, **2022**. *14*(6): p. 1049-1058. doi 10.1111/os.13238
15. Alomar, A.Z., et al., INTRAOPERATIVE EVALUATION AND LEVEL OF CONTAMINATION DURING TOTAL KNEE ARTHROPLASTY. *Acta Ortop Bras*, **2022**. *30*(spe1): p. e243232. doi 10.1590/1413-785220223001e243232
16. Khajanchi, B.K., et al., Immunomodulatory and protective roles of quorum-sensing signaling molecules N-acyl homoserine lactones during infection of mice with Aeromonas hydrophila. *Infect Immun*, **2011**. *79*(7): p. 2646-57. doi 10.1128/iai.00096-11
17. Thurlow, L.R., et al., Staphylococcus aureus biofilms prevent macrophage phagocytosis and attenuate inflammation in vivo. *J Immunol*, **2011**. *186*(11): p. 6585-96. doi 10.4049/jimmunol.1002794
18. Hanke, M.L., A. Angle, and T. Kielian, MyD88-dependent signaling influences fibrosis and alternative macrophage activation during Staphylococcus aureus biofilm infection. *PLoS One*, **2012**. *7*(8): p. e42476. doi 10.1371/journal.pone.0042476
19. Kristian, S.A., et al., Biofilm formation induces C3a release and protects Staphylococcus epidermidis from IgG and complement deposition and from neutrophil-dependent killing. *J Infect Dis*, **2008**. *197*(7): p. 1028-35. doi 10.1086/528992
20. Belgiovine, C., et al., Interaction of Bacteria, Immune Cells, and Surface Topography in Periprosthetic Joint Infections. *Int J Mol Sci*, **2023**. *24*(10) doi 10.3390/ijms24109028
21. Tucci, G., et al., Prevention of surgical site infections in orthopaedic surgery: a synthesis of current recommendations. *Eur Rev Med Pharmacol Sci*, **2019**. *23*(2 Suppl): p. 224-239. doi 10.26355/eurrev_201904_17497
22. Milleret, V., et al., Rational design and in vitro characterization of novel dental implant and abutment surfaces for balancing clinical and biological needs. *Clin Implant Dent Relat Res*, **2019**. *21 Suppl 1*: p. 15-24. doi 10.1111/cid.12736
23. Jeong, W.S., et al., Bacterial attachment on titanium surfaces is dependent on topography and chemical changes induced by nonthermal atmospheric pressure plasma. *Biomed Mater*, **2017**. *12*(4): p. 045015. doi 10.1088/1748-605X/aa734e
24. Skovdal, S.M., et al., Ultra-dense polymer brush coating reduces Staphylococcus epidermidis biofilms on medical implants and improves antibiotic treatment outcome. *Acta Biomater*, **2018**. *76*: p. 46-55. doi 10.1016/j.actbio.2018.07.002
25. Subramani, K., et al., Biofilm on dental implants: a review of the literature. *Int J Oral Maxillofac Implants*, **2009**. *24*(4): p. 616-26.

26. Savarino, L., et al., Biologic effects of surface roughness and fluorhydroxyapatite coating on osteointegration in external fixation systems: An in vivo experimental study. *J Biomed Mater Res A*, **2003**. *66A*(3): p. 652-661. doi https://doi.org/10.1002/jbm.a.10018
27. Scheeren Brum, R., et al., Early Biofilm Formation on Rough and Smooth Titanium Specimens: a Systematic Review of Clinical Studies. *J Oral Maxillofac Res*, **2021**. *12*(4): p. e1. doi 10.5037/jomr.2021.12401
28. Saulacic, N. and B. Schaller, Prevalence of Peri-Implantitis in Implants with Turned and Rough Surfaces: a Systematic Review. *J Oral Maxillofac Res*, **2019**. *10*(1): p. e1. doi 10.5037/jomr.2019.10101
29. Zeller, B., et al., Biofilm formation on metal alloys, zirconia and polyetherketoneketone as implant materials in vivo. *Clin Oral Implants Res*, **2020**. *31*(11): p. 1078-1086. doi 10.1111/clr.13654
30. Meier, D., et al., Biofilm formation on metal alloys and coatings, zirconia, and hydroxyapatite as implant materials in vivo. *Clin Oral Implants Res*, **2023**. *34*(10): p. 1118-1126. doi 10.1111/clr.14146
31. Hegde, V., et al., The Use of a Novel Antimicrobial Implant Coating In Vivo to Prevent Spinal Implant Infection. *Spine (Phila Pa 1976)*, **2020**. *45*(6): p. E305-e311. doi 10.1097/brs.0000000000003279
32. D'Almeida, M., et al., Chitosan coating as an antibacterial surface for biomedical applications. *PLoS One*, **2017**. *12*(12): p. e0189537. doi 10.1371/journal.pone.0189537
33. Asri, L.A.T.W., et al., A Shape-Adaptive, Antibacterial-Coating of Immobilized Quaternary-Ammonium Compounds Tethered on Hyperbranched Polyurea and its Mechanism of Action. *Adv Funct Mater*, **2014**. *24*(3): p. 346-355. doi https://doi.org/10.1002/adfm.201301686
34. Cao, Y., et al., Nanostructured titanium surfaces exhibit recalcitrance towards Staphylococcus epidermidis biofilm formation. *Sci Rep*, **2018**. *8*(1): p. 1071. doi 10.1038/s41598-018-19484-x
35. Albrektsson, T. and A. Wennerberg, On osseointegration in relation to implant surfaces. *Clin Implant Dent Relat Res*, **2019**. *21 Suppl 1*: p. 4-7. doi 10.1111/cid.12742
36. Voigt, J.D. and M. Mosier, Hydroxyapatite (HA) coating appears to be of benefit for implant durability of tibial components in primary total knee arthroplasty. *Acta Orthop*, **2011**. *82*(4): p. 448-59. doi 10.3109/17453674.2011.590762
37. Vidalain, J.P., Twenty-year results of the cementless Corail stem. *Int Orthop*, **2011**. *35*(2): p. 189-94. doi 10.1007/s00264-010-1117-2
38. Røkkum, M., A. Reigstad, and C.B. Johansson, HA particles can be released from well-fixed HA-coated stems: histopathology of biopsies from 20 hips 2-8 years after implantation. *Acta Orthop Scand*, **2002**. *73*(3): p. 298-306. doi 10.1080/000164702320155293
39. Overgaard, S., et al., Improved fixation of porous-coated versus grit-blasted surface texture of hydroxyapatite-coated implants in dogs. *Acta Orthop Scand*, **1997**. *68*(4): p. 337-43. doi 10.3109/17453679708996173
40. Nunes, F., et al., Effect of Smoke Exposure on Gene Expression in Bone Healing around Implants Coated with Nanohydroxyapatite. *Nanomaterials (Basel)*, **2022**. *12*(21) doi 10.3390/nano12213737
41. Adam, M., et al., In vivo and in vitro investigations of a nanostructured coating material - a preclinical study. *Int J Nanomedicine*, **2014**. *9*: p. 975-84. doi 10.2147/ijn.S48416
42. Johansson, P., et al., Nanosized Hydroxyapatite Coating on PEEK Implants Enhances Early Bone Formation: A Histological and Three-Dimensional Investigation in Rabbit Bone. *Materials (Basel)*, **2015**. *8*(7): p. 3815-3830. doi 10.3390/ma8073815
43. Almeida, D., et al., In vivo osseointegration evaluation of implants coated with nanostructured hydroxyapatite in low density bone. *PLoS One*, **2023**. *18*(2): p. e0282067. doi 10.1371/journal.pone.0282067
44. Bergamo, E.T.P., et al., Osseointegration of implant surfaces in metabolic syndrome and type-2 diabetes mellitus. *J Biomed Mater Res B Appl Biomater*, **2024**. *112*(2): p. e35382. doi 10.1002/jbm.b.35382
45. Johansson, P., et al., Polyether ether ketone implants achieve increased bone fusion when coated with nano-sized hydroxyapatite: a histomorphometric study in rabbit bone. *Int J Nanomedicine*, **2016**. *11*: p. 1435-42. doi 10.2147/ijn.S100424
46. Moris, V., et al., What is the best technic to dislodge Staphylococcus epidermidis biofilm on medical implants? *BMC Microbiol*, **2022**. *22*(1): p. 192. doi 10.1186/s12866-022-02606-x

47. Karbysheva, S., et al., Comparison of sonication with chemical biofilm dislodgement methods using chelating and reducing agents: Implications for the microbiological diagnosis of implant associated infection. *PLoS One*, **2020**. *15*(4): p. e0231389. doi 10.1371/journal.pone.0231389
48. Guerreiro-Tanomaru, J.M., et al., Effect of addition of nano-hydroxyapatite on physico-chemical and antibiofilm properties of calcium silicate cements. *J Appl Oral Sci*, **2016**. *24*(3): p. 204-10. doi 10.1590/1678-775720150422
49. Lamkhao, S., et al., Synthesis of Hydroxyapatite with Antibacterial Properties Using a Microwave-Assisted Combustion Method. *Sci Rep*, **2019**. *9*(1): p. 4015. doi 10.1038/s41598-019-40488-8
50. Ragab, H., et al., Synthesis and In Vitro Antibacterial Properties of Hydroxyapatite Nanoparticles. *IOSR J Pharm Biol Sci*, **2014**. *9*: p. 77-85. doi 10.9790/3008-09167785
51. Park, M., J.B. Sutherland, and F. Rafii, Effects of nano-hydroxyapatite on the formation of biofilms by Streptococcus mutans in two different media. *Arch Oral Biol*, **2019**. *107*: p. 104484. doi https://doi.org/10.1016/j.archoralbio.2019.104484
52. Grenho, L., et al., Adhesion of Staphylococcus aureus, Staphylococcus epidermidis, and Pseudomonas aeruginosa onto nanohydroxyapatite as a bone regeneration material. *J Biomed Mater Res A*, **2012**. *100*(7): p. 1823-30. doi 10.1002/jbm.a.34139
53. Abdulkareem, E.H., et al., Anti-biofilm activity of zinc oxide and hydroxyapatite nanoparticles as dental implant coating materials. *J Dent*, **2015**. *43*(12): p. 1462-1469. doi https://doi.org/10.1016/j.jdent.2015.10.010
54. Zakrzewski, W., et al., Antimicrobial Properties and Cytotoxic Effect Evaluation of Nanosized Hydroxyapatite and Fluorapatite Dedicated for Alveolar Bone Regeneration. *Appl Sci*, **2024**. *14*(17): p. 7845.
55. Whyte, W., et al., Suggested bacteriological standards for air in ultraclean operating rooms. *Journal of Hospital Infection*, **1983**. *4*(2): p. 133-139. doi https://doi.org/10.1016/0195-6701(83)90042-7
56. Lidwell, O.M., Airborne bacteria and surgical infection. *The American Journal of Medicine*, **1981**. *70*(3): p. 693-697. doi https://doi.org/10.1016/0002-9343(81)90598-2
57. Stocks, G.W., et al., Predicting bacterial populations based on airborne particulates: A study performed in nonlaminar flow operating rooms during joint arthroplasty surgery. *American Journal of Infection Control*, **2010**. *38*(3): p. 199-204. doi https://doi.org/10.1016/j.ajic.2009.07.006
58. Guarch-Pérez, C., et al., Bacterial reservoir in deeper skin is a potential source for surgical site and biomaterial-associated infections. *Journal of Hospital Infection*, **2023**. *140*: p. 62-71. doi https://doi.org/10.1016/j.jhin.2023.07.014
59. Granato, R., et al., Clinical, histological, and nanomechanical parameters of implants placed in healthy and metabolically compromised patients. *J Dent*, **2020**. *100*: p. 103436. doi 10.1016/j.jdent.2020.103436
60. Baskar, K., T. Anusuya, and G. Devanand Venkatasubbu, Mechanistic investigation on microbial toxicity of nano hydroxyapatite on implant associated pathogens. *Mat Sci Eng C*, **2017**. *73*: p. 8-14. doi https://doi.org/10.1016/j.msec.2016.12.060
61. Knabel, S.J., H.W. Walker, and P.A. Hartman, Inhibition of Aspergillus flavus and Selected Gram-positive Bacteria by Chelation of Essential Metal Cations by Polyphosphates. *J Food Prot*, **1991**. *54*(5): p. 360-365. doi https://doi.org/10.4315/0362-028X-54.5.360
62. Xie, Y. and L. Yang, Calcium and Magnesium Ions Are Membrane-Active against Stationary-Phase Staphylococcus aureus with High Specificity. *Sci Rep*, **2016**. *6*(1): p. 20628. doi 10.1038/srep20628
63. Shao, H., et al., Advances in the superhydrophilicity-modified titanium surfaces with antibacterial and pro-osteogenesis properties: A review. *Front Bioeng Biotechnol*, **2022**. *10*: p. 1000401. doi 10.3389/fbioe.2022.1000401
64. Kinnari, T.J., et al., Influence of surface porosity and pH on bacterial adherence to hydroxyapatite and biphasic calcium phosphate bioceramics. *J Med Microbiol*, **2009**. *58*(Pt 1): p. 132-137. doi 10.1099/jmm.0.002758-0